Structural Engineering and Mechanics, Vol. 4, No. 3 (1996) 313-329
DOI: http://dx.doi.org/10.12989/sem.1996.4.3.313

Extension of a cable in the presence of dry friction

Xiaolun Huang†

Wittke Waste Equipment, Medicine Hat, AB, T1C 1K6 Canada

Oleg G. Vinogradov‡

Department of Mechanical Engineering, University of Calgary, Calgary, AB, T2N 1N4 Canada

Abstract. A mathematical model of a cable as a system of interacting wires with interwire friction taken into account is presented in this paper. The effect of friction forces and the interwire slip on the mechanical properties of tension cables is investigated. It is shown that the slip occurs due to the twisting and bending deformations of wires, and it occurs in the form of micro-slips at the contact patches and macro-slips along the cable. The latter slipping starts near the terminals and propagates towards the middle of the cable with the increase of tension, and its propagation is proportional to the load. As the result of dry friction, the load-elongation characteristics of the cable become quadratic. The energy losses during the extension are shown to be proportional to the cube of the load and in inverse proportion to the friction force, a result qualitatively similar to that for lap joints. Presented examples show that the model is in qualitative agreement with the known experimental data.

Key words: cable mechanics; energy losses; interwire friction.

1. Introduction

Cables are commonly used as tension members in large space engineering structures such as suspension bridges and large-span roofs, in mooring systems, in concrete reinforcement, etc. In all applications where the cyclic deformations are taking place, the damping properties of the cables and their effect on the dynamic behaviour of structures is of interest (Vranish, 1990).

It is known that dry friction is the main cause of damping in cables, since it is much larger than the material viscosity (Pipes 1936, Yu 1952, Claren and Diana 1969, Vinogradov and Pivovarov 1986). However, the integration of friction forces into the cable mechanics remains a challenging problem today. In most of the theoretical studies on cables subjected to axial loads, the interwire friction was neglected (Machida and Durelli 1973, Chi 1974, Phillips and Costello 1977, Knapp 1979, Kumar and Cochran 1987). As a result, these friction-free models of cables are unable to simulate their damping properties.

A widely accepted approach in cable mechanics is to consider a cable as an assembly of helical thin rods. Within the framework of this approach, the interwire friction forces can be treated as externally distributed loads in the form of forces and/or moments acting on each wire in the cable. However, the cause of these forces, namely, the interwire slippage, very often

† Mechanical Engineer
‡ Professor

is not taken into account (LeClair and Costello 1988). The slipping behaviour and energy dissipation in a bent cable in the presence of interwire dry friction were investigated by Vinogradov and Atatekin (1986) and Huang and Vinogradov (1994). In the case of an axially loading cable, Huang (1978) included the interwire friction effects in his analysis of the finite extension of a uniformly stretched cable. The effect of interwire friction and slip in a stretched cable was also investigated theoretically and experimentally by Utting and Jones (1987). Ramsey (1990) in his analytical study found that in a uniformly stretched cable the interwire friction will occur only in a form of moments balancing the change of the helix angle. More recently, Huang and Vinogradov (1992) extended their theoretical model on the extension of the cable with interwire friction to predict its energy losses in a cyclic loading.

The focus of this paper is the study of cable extension in the presence of interwire friction and associated slip. In the following sections, basic equations of the thin rod theory related to our analysis are first reviewed. Then the kinematic relationships, including a criterion for slip prediction, are presented. The expressions for the slipping length are derived in an explicit form as functions of load and cable parameters, such as the helix angle and the number of wires. Finally, an expression for the extension of the cable in the presence of finite friction is presented. The experimental data of Utting and Jones (1987) are used to qualitatively validate the obtained theoretical results.

2. Analysis

A cable is considered here as a single strand formed by an arbitrary number of helical wires wound around the core. An eight-wire cable, for example, is shown in Fig. 1. This model allows to simplify the mathematical analysis without losing the characteristic properties associated with the interwire friction, slip and corresponding energy losses. As in most engineering applications, a cable is considered to be fixed at both ends in order to prevent the self-loosening twist, and

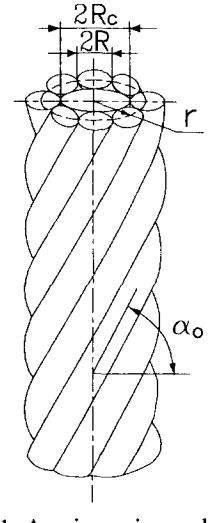

Fig. 1 A nine-wire cable.

the cable's deformations are assumed to be elastic and small. Also, a dry friction at the interfaces and a constant coefficient of friction is assumed. The latter is based on the observation that the interwire contact forces are usually dominated by the pre-stretching (static) load which is much larger than the amplitude of the dynamic load. The local effects at the clamping ends are neglected. Due to symmetry, only a half of the cable is considered, so that the middle of the cable is fixed and the extension is applied at the clamped end.

2.1. Basic equations for a thin-rod model of cable

Each wire in the cable is treated as a thin rod and its initial shape is assumed to be a helix. Accordingly, the displacement of the wire cross-section is described by a translational component along the wire centerline and three rotational components. The orientations of the wire cross-section can be described by a triad ($\boldsymbol{t}$, $\boldsymbol{n}$, $\boldsymbol{b}$) moving along the wire centerline, as shown in Fig. 2, in which $\boldsymbol{t}$, $\boldsymbol{n}$ and $\boldsymbol{b}$ are unit vectors indicating the tangential, normal and binormal directions of the helical line, respectively.

Denote the internal force components in the tangential, normal and binormal directions by F_t, F_n and F_b, the external distributed forces acting on the wire by p_t, p_n and p_b, and the external distributed moments by m_t, m_n and m_b, respectively. Then the equilibrium equations for the wire according to (Huang 1973) are

$$\frac{dF_t}{ds}-\kappa' F_n+p_t=0 \tag{1}$$

$$\frac{dF_n}{ds}-\tau F_b+\kappa' F_t+p_n=0 \tag{2}$$

$$\frac{dF_b}{ds}+\tau F_n+p_b=0 \tag{3}$$

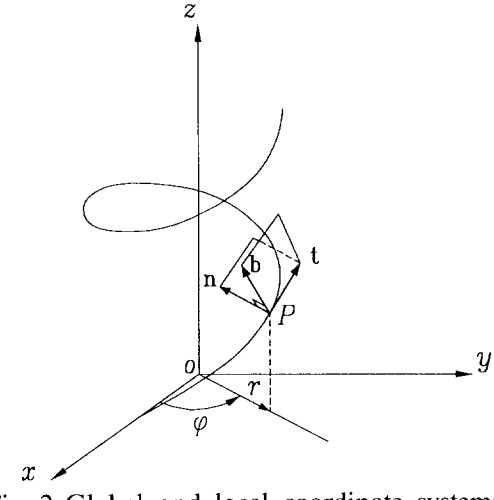

Fig. 2 Global and local coordinate systems.

$$\frac{dM_t}{ds} - \kappa' M_n + m_t = 0 \tag{4}$$

$$\frac{dM_n}{ds} - \tau M_b + \kappa' M_t - F_b + m_n = 0 \tag{5}$$

$$\frac{dM_b}{ds} + \tau M_n + F_n + m_b = 0 \tag{6}$$

If the helix angle and helix radius of the wire in an initial state are denoted by α_0 and r_0, respectively, then the torsion (τ_0) and curvatures (κ_0 and κ_0') for the wire can be defined by (Love 1944)

$$\tau_0 = \frac{\sin 2\alpha_0}{2r_0}, \quad \kappa_0 = 0, \quad \kappa_0' = \frac{\cos^2\alpha_0}{r_0} \tag{7}$$

Similarly, if the helix angle and helix radius of the wire after deformation are denoted by α and r, the new geometry of the wire is given by[c]

$$\tau = \frac{\sin 2\alpha}{2r}, \quad \kappa = -\frac{d\alpha}{ds}, \quad \kappa' = \frac{\cos^2\alpha}{r} \tag{8}$$

The axial force component, F_t, is proportional to the axial strain ε_t, so that

$$F_t = A\varepsilon_t \tag{9}$$

where $A = E\pi R^2$, R is the radius of the wire cross-section, E is Young's modulus of the wire material.

According to the Clensch-Basset moment-curvature formula (Love 1944), the three components of the internal moment in a wire cross-section, M_t, M_n and M_b, are related to the change in the torsion and bending curvatures by

$$M_t = \frac{B}{1+\nu}(\tau - \tau_0), \qquad M_n = B(\kappa - \kappa_0), \; M_b = B(\kappa' - \kappa'_0) \tag{10}$$

where $B = E\pi R^4/4$, ν is Poisson ratio of the wire material.

If the radius of the core cross-section is denoted by R_c, the helix radius for the wire in touch with the core is given by $r_0 = R_c + R$. It is reasonable to represent r by r_0, since the error caused by neglecting the contact and lateral shrinkage of the wire under the axial extension is within 1% (Utting and Jones 1987). Also from the assumption of small deformations, the change of the helix angle, denoted by $\Delta\alpha = \alpha - \alpha_0$, is small as well. As a result, Eq. (10) after substituting Eqs. (7)-(8) into it, can be represented by

$$M_t = \frac{B}{1+\nu}\frac{\cos 2\alpha_0}{r}\Delta\alpha, \quad M_n = -B\frac{d\alpha}{ds}, \quad M_b = -B\frac{\sin 2\alpha_0}{r}\Delta\alpha \tag{11}$$

From the geometry of an elementary length of the developed helical wire (see Fig. 3) in its

[c] According to Love (1994, p. 383), the torsion of a thin rod consists of two components: the rotation of the cross section moving along with the twisted centerline and the rotation of the cross section around the centerline (df/ds). Because $\tan f = -(k'/k)$ (Love, Eq. 3, p. 383), it can be shown that $df/ds = -k^2 \sin 2\alpha/[r(k^2+k'^2)]$ is a second order term and thus is neglected.

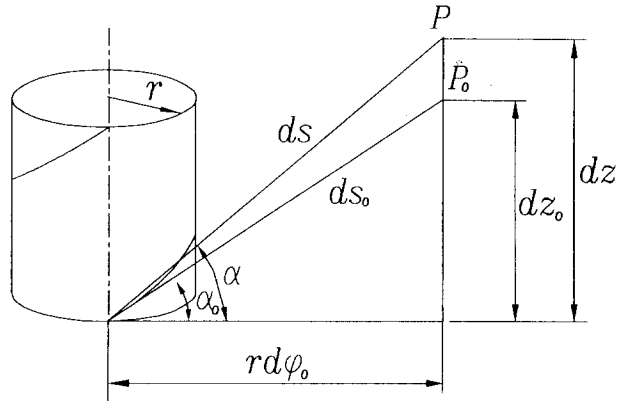

Fig. 3 Development of an elementary helix length for two deformation states: initial, indicated by subscript 0, and intermediate state.

initial and deformed states, we can obtain the following relationship between the axial strain ε_t of the wire and its component along the cable axis, ε_c. That is

$$\varepsilon_t=\frac{\sin\alpha_0}{\sin\alpha}(1+\varepsilon_c)-1 \tag{12}$$

It follows from the fixed-end condition that the centerline of a helical wire has no rotational movement with respect to the cable axis, i.e. the polar coordinates of the wire do not change (see Fig. 3)

$$\frac{r_0}{r}\frac{1+\varepsilon_c}{\tan\alpha}-\frac{1}{\tan\alpha_0}=0 \tag{13}$$

For the case of small deformations, Eq. (13) is reduced to

$$\Delta\alpha=-\frac{\sin2\alpha_0}{2}\varepsilon_c \tag{14}$$

Solving Eqs. (12) and (14) together, the axial strain in the helical wire is found to be a function of the change of the helix angle in the form

$$\varepsilon_t=\Delta\alpha\tan\alpha_0 \tag{15}$$

As it is shown in Eqs. (9), (10) and (15), the internal force F_t and moments M_t, M_n and M_b are also expressed as functions of $\Delta\alpha$.

2.2. Extension of the friction-free cable

To understand how an interwire slip occurs inside a cable, it is helpful to consider first the deformations and forces in the cable under friction-free conditions, a commonly used assumption in theoretical analyses of cable extension. Since for the friction-free conditions $p_t=p_b=m_t=m_n=m_b=0$, the equilibrium equations, Eqs. (1)-(6), become

$$F_n = \frac{d\alpha}{ds} = 0 \tag{16}$$

and

$$F_b = \frac{B}{r^2}\left(\frac{\sin^2 2\alpha_0}{2} + \frac{\cos^2\alpha_0 \cos 2\alpha_0}{1+\nu}\right)\Delta\alpha \tag{17}$$

Also, under the friction-free assumption, the strain in the core is constant along the cable and thus must be equal to the strain component of the helical wire in the direction of the cable axis, given by Eq. (14), in order to satisfy the compatibility conditions of elongation. Thus the internal force in the core can be written as

$$F_c = -\frac{2A_c \Delta\alpha}{\sin 2\alpha_0} \tag{18}$$

where $A_c = E_c \pi R_c^2$. Substituting the forces and moments given by Eqs. (9), (10), and (16)-(18) into the following equilibrium equation

$$P = F_c + n(F_t \sin\alpha + F_b \cos\alpha) \tag{19}$$

we can find that the change of the helix angle is proportional to the extension force

$$\Delta\alpha = CP \tag{20}$$

where

$$C = \left[-\frac{2A_c}{\sin 2\alpha_0} + nA \tan\alpha_0 \sin\alpha_0 + \frac{nB}{r^2}\cos^3\alpha_0\left(2\sin^2\alpha_0 + \frac{\cos 2\alpha_0}{1+\nu}\right)\right]^{-1} \tag{21}$$

2.3. Slip in the friction-free cable

Like in a helical spring, extension of the helical wire in a cable is always associated with twisting (around unit vector t) and bending (around unit vectors n and b) deformations of the cross sections. In the following the relative displacements at the interface between the helical wire and core are found. For an infinitesimal length of the helical wire, the displacement along the direction of the cable axis is given by

$$du_z^w = \varepsilon_c dz + R\left[\frac{M_t}{B}(1+\nu)\cos\alpha - \frac{M_b}{B}\sin\alpha\right]ds \tag{22}$$

The latter can be reduced, after using Eqs. (11), (14) and taking that $ds \approx dz/\sin\alpha_0$, to

$$du_z^w = \left(1 + \frac{R}{r}\cos^2\alpha_0\right)\frac{\Delta\alpha}{\cos\alpha_0}ds \tag{23}$$

The rotational displacement of the wire with respect to the core is given by

$$du_r^w = R\left(\frac{M_t}{B}(1+\nu)\sin\alpha + \frac{M_b}{B}\cos\alpha\right) \tag{24}$$

which can also be reduced to

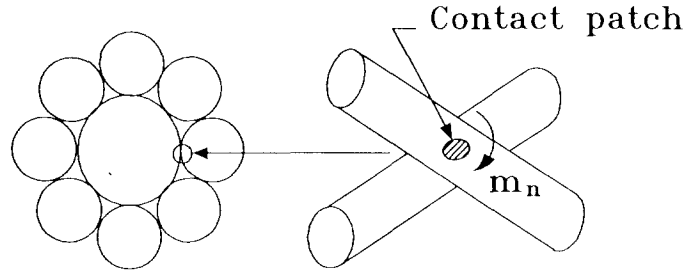

Fig. 4 Micro-slip at a contact patch.

$$du_r^w = -\frac{R}{r}\sin\alpha_0 \Delta\alpha ds \tag{25}$$

The rotation of the wire given by Eq. (25) indicates that since the core has no rotational displacement under the friction-free conditions slip must occur inside the cable.

2.4. Uniform extension of the cable with friction

The assumption of a uniform deformation leads to a constant helix angle along the cable. It follows that the case of cable extension in the presence of friction can be solved similarly to that of the friction-free cable. As a result, the following is found

$$F_n = 0, \qquad p_t = p_b = m_t = m_b = 0 \tag{26}$$

$$F_b = m_n + \frac{B}{r^2}\left(\frac{\sin^2 2\alpha_0}{2} + \frac{\cos^2\alpha_0 \cos 2\alpha_0}{1+\nu}\right)\Delta\alpha \tag{27}$$

$$\Delta\alpha = C(P - nm_n\cos\alpha_0) \tag{28}$$

The friction moment m_n is due to the shear force at the contact patch between the wires and the core (see Fig. 4). The corresponding friction losses are due to rotation of the wire cross-section around vector n. The associated slip is uniform along the cable length since it is proportional to $\Delta\alpha$ to which is the same for any cross-section in a uniformly extended cable. This slip is called here a *micro-slip* since it takes place locally at the contact patch (see Fig. 4). The corresponding friction work per unit length of a helical wire is given by

$$w_a = m_n \Delta\alpha \tag{29}$$

2.5. Extension of the cable with absolute friction

The condition of absolute friction means that the interwire friction forces could be as large as the shear forces at the interface. Under such conditions any slip will be prevented and a cable will behave like a solid bar. In this case the tensile stiffness can be approximated by

$$K_n = A_c + \frac{nA}{\sin\alpha_0} \tag{30}$$

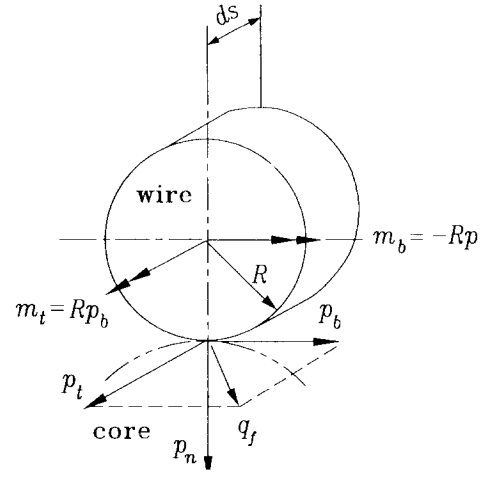

Fig. 5 Interwire forces.

and the axial strain will be equal to

$$\varepsilon_{cn}=\frac{P}{K_n} \tag{31}$$

while the helix angle, after substituting Eq. (31) into (14), will become

$$\alpha_n=\alpha_0+\frac{\sin 2\alpha_0}{2}\frac{P}{K_n} \tag{32}$$

2.6. Extension of the cable with finite friction and slip

Since friction in a real cable can only be finite, a slip associated with rotations of the wire cross-sections around vectors t and b (twisting and bending deformations) will occur if the interwire shear force exceeds the friction limit. As shown in Fig. 5, the interwire friction moments are related to the friction forces by

$$m_t=Rp_b, \qquad m_b=-Rp_t \tag{33}$$

Then from the equilibrium equations, Eqs. (1)-(6), the following can be found

$$p_t=c_1\frac{d\alpha}{ds}, \qquad p_b=c_2\frac{d\alpha}{ds} \tag{34}$$

$$F_n=c_3\frac{d\alpha}{ds}, \qquad F_b=c_4\Delta\alpha \tag{35}$$

where

$$c_1=\frac{A\tan\alpha_0-\dfrac{3B}{r^2}\sin\alpha_0\cos^3\alpha_0}{\dfrac{R}{r}\cos^2\alpha_0-1} \tag{36}$$

$$c_2=-\frac{B}{Rr}\left(\frac{\cos 2\alpha_0}{1+\nu}+\cos^2\alpha_0\right) \tag{37}$$

$$c_3=Rc_1+\frac{3B}{2r}\sin 2\alpha_0 \tag{38}$$

$$c_4=-\left(c_2+\frac{\sin 2\alpha_0}{2r}c_3\right) \tag{39}$$

If the interwire friction limit is denoted by p_f, then the criterion of slipping is

$$p_f^2=p_t^2+p_b^2 \tag{40}$$

or, after substituting Eq. (34),

$$p_f=\sqrt{c_1^2+c_2^2}\frac{d\alpha}{ds} \tag{41}$$

Thus, in the presence of slippage, the change of the helix angle is governed by the equation

$$\frac{d\alpha}{ds}=Dp_f \tag{42}$$

where

$$D=\frac{1}{\sqrt{c_1^2+c_2^2}} \tag{43}$$

It follows from the symmetry of the cable structure that neither the helical wire nor the core will rotate at the middle of the cable. However, away from the middle, as the twisting and bending stresses in the wire increase the friction forces might be overcome and then the slippage will take place. This slippage will originate in the parts of the cable close to the ends and spread along some length towards the middle of the cable. This slip is called here a *macro-slip* since it takes place along some length and is not uniform along the cable. The macro-slip is similar to propagation of the slip boundary in lap joints (Goodman, 1959). Thus the extended cable will consist of two segments: with uniform and nonuniform deformations. In the segment with uniform deformations the interwire slip does not take place. Whereas in the segment with nonuniform deformations the helix angle α will vary and the interwire slip must occur. This slip will comprise both micro- and macro-components. In the slipping segment the axial force F_c^* and the twisting moment M_c^* in the core are given by

$$F_c^*=F_c+n\int_0^{s(z)}(p_t\sin\alpha+p_b\cos\alpha)\,ds \tag{44}$$

$$M_c^*=M_c+n\int_0^{s(z)}(p_t\cos\alpha-p_b\sin\alpha)\,ds \tag{45}$$

where the arc length s is measured from the boundary between the uniform and slipping segments towards the cable end. The axial and rotational displacements of an infinitesimal length of the core in the slipping segment are defined by,based on Eqs. (44) and (45) and using the results

in Eq. (34),

$$du_z^c=\left(\frac{F_c}{A_c}+\frac{n}{A_c}\,c_5\Delta\alpha_s\right)dz \tag{46}$$

$$du_r^c=\frac{1+\nu_c}{B_c}\,R_c(M_c+nR_c c_6\Delta\alpha_s)\,dz \tag{47}$$

where $\Delta\alpha_s=\alpha_s-\alpha$ and

$$c_5=c_1\sin\alpha_0+c_2\cos\alpha_0 \tag{48}$$

$$c_6=c_1\cos\alpha_0-c_2\sin\alpha_0 \tag{49}$$

From the boundary conditions that when $\alpha_s=\alpha$, then $du_z^w=du_z^c$ and $du_r^w=-du_r^c$ at the boundary between the uniform and slipping segments, and using Eq. (23) to Eq. (46) and Eq. (25) to (47), it is obtained

$$F_c=\left(1+\frac{R}{r}\cos^2\alpha_0\right)\frac{2A_c\Delta\alpha}{\sin2\alpha_0} \tag{50}$$

$$M_c=\frac{R}{rR_c}\,\frac{B_c}{1+\nu_c}\,\Delta\alpha \tag{51}$$

The length of the slipping segment, denoted by H_s, can be found from the condition that the rotational displacement of the core at the fixed end is equal to zero. The change of the helix angle in the slipping segment, $\Delta\alpha_s$, can be found from Eq. (42) to be as follows

$$\Delta\alpha_s=\frac{Dp_f z}{\sin\alpha_0} \tag{52}$$

Now the slipping length H_s can be found, using Eqs. (47), (51) and (52) and the boundary condition that $u_r^c=0$ at $z=H_s$, to be

$$H_s=-\frac{RA_c}{2nrc_6Dp_f(1+\nu_c)}\sin\alpha_0\Delta\alpha \tag{53}$$

Note that c_6 is always negative so that it ensures that the physical meaning of H_s is correct.

The energy dissipation rate per unit length of the wire inside the slipping segment H_s is defined by

$$\frac{dw_s}{dz}=\left(\frac{du_z^w}{dz}-\frac{du_z^c}{dz}\right)(p_t\sin\alpha+p_b\cos\alpha)+\left(\frac{du_r^w}{dz}+\frac{du_r^c}{dz}\right)(p_t\cos\alpha-p_b\sin\alpha) \tag{54}$$

The latter can be reduced, after substituting Eqs. (23), (25), (46)-(49) and (52), to

$$w_s=nc_7(Dp_f)^2z^2 \tag{55}$$

where

$$c_7=\frac{1}{2A_c\sin\alpha_0}\,[c_5^2+4(1+\nu_c)c_6^2] \tag{56}$$

The extension of the cable of length $2H$ as a function of the increasing tensile load P is

calculated in two steps:

(1) $0 < P \leq nm_n \cos\alpha_0$. The middle part of the cable with the length of $2(H-H_s)$ is in a non-slipping situation, and the change of the helix angle is equal to $\Delta\alpha_n$, given by Eq. (32). At the same time, the length of the slipping segment, H_s, can be found from Eq. (53) by substituting $\Delta\alpha = \Delta\alpha_s$. The total elongation is the sum of contributions from the slipping and non-slipping segments and is given by Eq. (14).

$$\delta = \frac{4}{\sin 2\alpha_0}\left(\int_0^H \Delta\alpha_n dz + \int_0^{H_s} \Delta\alpha_s dz\right) \tag{57}$$

which will yield, after using Eqs. (14), (32) and (52).

$$\delta = \frac{2H}{K_n} P + \frac{Dp_f}{\sin^2\alpha_0 \cos\alpha_0} H_s^2 \tag{58}$$

In the extreme case when the interwire friction p_f is infinite, the second term in the above equation will vanish since the slipping length H_s equals to zero in Eq. (53). Then, as expected, a cable will behave like a solid bar.

(2) $P > nm_n \cos\alpha_0$. The middle part of the cable will experience a uniform extension with a micro-slip at the contact patch and rolling displacement between the helical wires and the core. The corresponding change in the helix angle, $\Delta\alpha$, is given by Eq. (28), and the extension is as follows

$$\delta = \frac{2H}{K_n} nm_n \cos\alpha_0 + \frac{4}{\sin 2\alpha_0}\left(\int_0^H \Delta\alpha dz + \int_0^{H_s} \Delta\alpha_s dz\right) \tag{59}$$

which, as in the previous case, is transformed to

$$\delta = \frac{2H}{K_n} nm_n \cos\alpha_0 + \frac{4HC}{\sin 2\alpha_0}(P - nm_n \cos\alpha_0) + \frac{Dp_f}{\sin^2\alpha_0 \cos\alpha_0} H_s^2 \tag{60}$$

It is seen that the elongation of the cable with interwire slip, given by Eqs. (58) and (60), is a non-linear function of the axial load. It should be pointed out that Eq. (53) is valid only if the length of slipping segments does not exceed the cable length, the condition applicable to long cables. As shown in Eq. (53), the slipping length is in inverse proportion to the friction force p_f. But the ultimate length of the slipping segments is the cable length. If the friction is equal to zero, the entire cable will be under uniform extension, and the elongation defined by Eq. (60) will yield the same result as that for the friction-free cable.

When the load is within the limits $0 < P \leq nm_n \cos\alpha_0$, the energy dissipation for the entire cable is given by

$$W_f = 2n \int_0^{H_s} w_s dz \tag{61}$$

The latter, after substitution of Eqs. (32), (53) and (55), becomes

$$W_f = \frac{c_8}{p_f}\left(\frac{\sin 2\alpha_0}{2K_n}\right)^3 P^3 \tag{62}$$

where

$$c_8 = -\frac{c_7}{12nD}\left[\frac{RA_c \sin\alpha_0}{rc_6(1+\nu_c)}\right]^3 \tag{63}$$

When the load $P \geq nm_n \cos\alpha_0$, the energy dissipation is given by

$$W_f = 2n\int_0^H w_\alpha dz + 2n\int_0^{H_s} w_s dz \tag{64}$$

which after substitution of Eqs. (28), (53) and (55) yilds

$$W_f = 2Hnm_n C(P - nm_n \cos\alpha_0) + \frac{c_8 C^3}{p_f} P^3 \tag{65}$$

3. Examples and discussion

In this section a new mathematical model of a cable with finite friction forces is discussed and evaluated through some numerical examples. In order to compare the numerical results with the experimental ones reported by Utting and Jones (1987), the following data for a single layered cable will be used: $n=6$, $R_c=1.97$ mm, $R=1.865$ mm, $\alpha_0=76.16°$, $H=0.75$ m, $E=E_c=197.9$ GPa, $\nu=\nu_c=0.3$, and the interwire distributed friction force p_f and moment m_n are assumed to be constant and equal to 1 kN/m and 100 N-m/m, respectively, except where they are specified.

3.1. Slip propagation

First, it should be pointed out that there is no direct experimental evidence on the propagation of the macro-slip in cables during the axial loading. It is possible that no attempt has been made to find it, but more likely it is not easy to confirm it because of the complex and non-ideal geometry of the wire assembly. The fact is that in real cables the axial load is unevenly

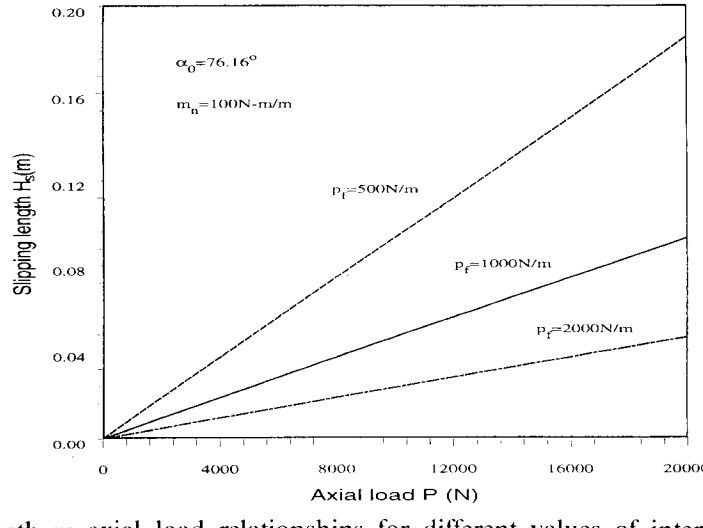

Fig. 6 Slipping length *vs* axial load relationships for different values of interwire friction forces.

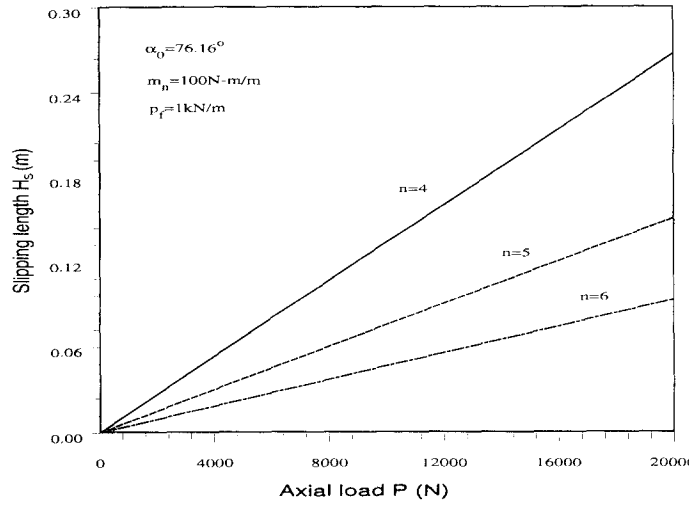

Fig. 7 Slipping length *vs* axial load relationship for different number of wires.

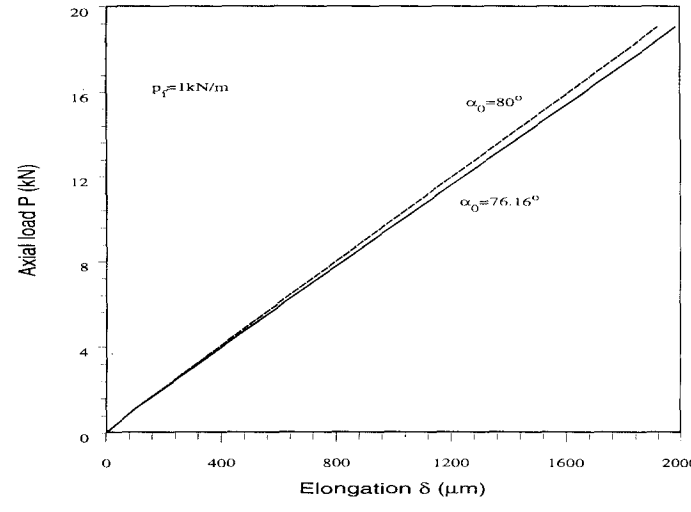

Fig. 8 Axial load *vs* cable elongation relationship for two values of helix angles.

shared between the wires (Cappa 1987). There are also indications that the contact forces (and thus the friction forces) are uneven along the cable (Casey and Lee 1989). It is known, however, that the temperature of the cable under cyclic loading is usually higher near the clamps. This is an indication of the presence of slippage that causes the heat. Also the presented theory of macro-slip propagation is in agreement with analogous phenomenon in lap joints. Eq. (53) shows that the propagation of the macro-slip is proportional to the change of the helix angle, which, in turn (Eqs. (20), (28) and (32)), is proportional to the axial loading. The slip propagates faster in the case of smaller interwire friction forces (smaller pre-tension and/or friction coefficient) and fewer helical wires. This can be seen in Figs. 6 and 7 of the numerical examples.

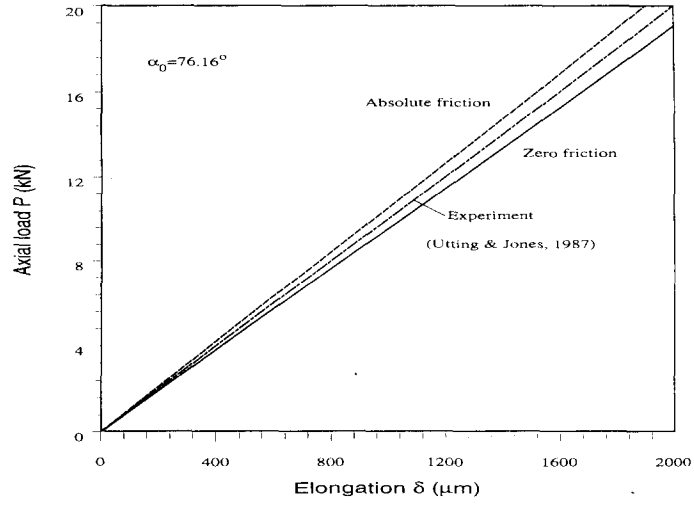

Fig. 9 Comparison of the load-elongation relationships from the theory and experiment.

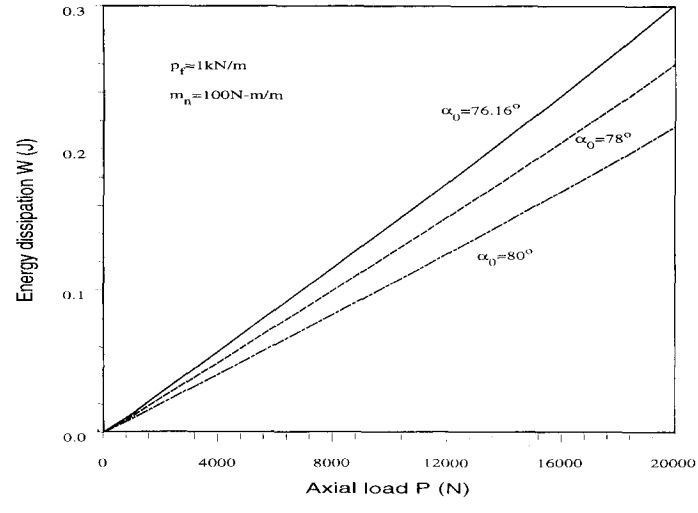

Fig. 10 Energy dissipation *vs* axial load for different helix angles.

3.2. Cable elongation vs axial load

The present model shows that the elongation of the cable is a nonlinear function of the axial load. The nonlinearity, however, is usually small so that it may be ignored in engineering applications. This is seen in Fig. 8 where the load *vs* elongation curves are shown for two values of helix angles. In an extreme situation when the interwire friction is zero, the present model becomes nearly identical to the Costello's (1990) model (not shown in the figure). The slight difference is attributed to the fact that in the present model the Poisson's ratio effect on the change of the transverse dimension of the wires was ignored.

In Fig. 9 two boundaries of the model are shown: absolute and zero friction conditions. It

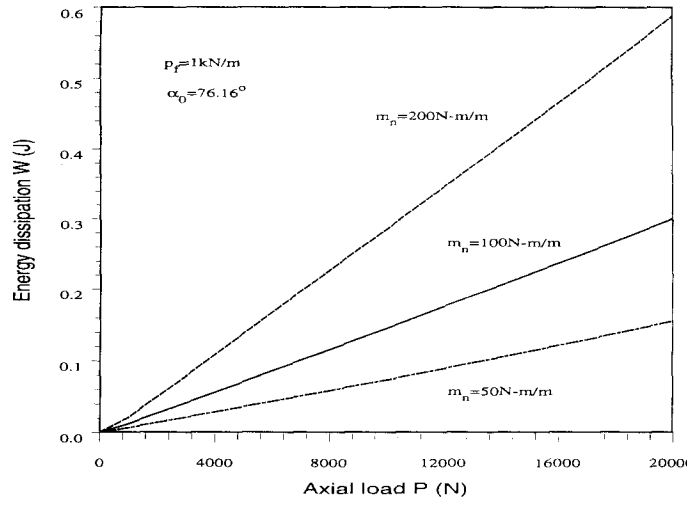

Fig. 11 Energy dissipation *vs* axial load for different friction moments.

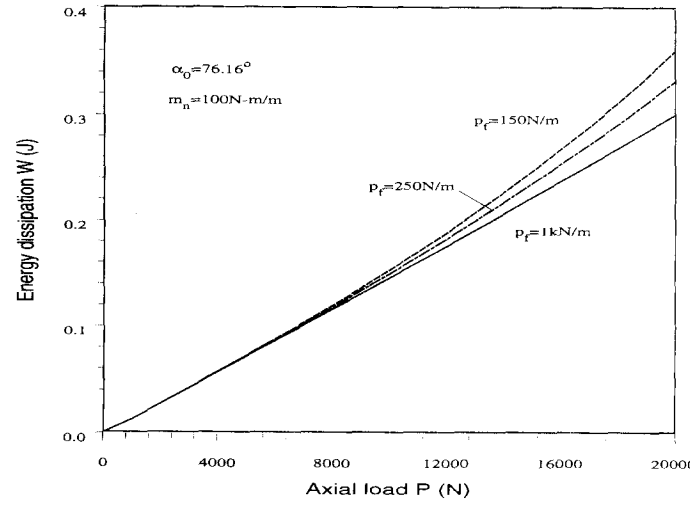

Fig. 12 Energy dissipation *vs* axial load for different friction forces.

is seen that the experimental results by Utting and Jones (1987) are bounded by the two extremes. The validity of the present model is further confirmed by noting that for the magnitude of the interwire friction moment 50N-m/m, found by trial, the theoretical curve coincides with the experimental one.

3.3. Energy dissipation

Energy dissipation presented by Eqs. (62) and (65) shows that it consists of two parts: one is proportional to both the axial load and the interwire friction moments, and another is proportional to the cube of the axial load but is in inverse proportion to the interwire friction forces.

The former is due to the micro-slip at the contact patches. The latter is the result of the macro-slip propagating along the cable, which is qualitatively similar to the slip in lap joins with dry friction (Goodman, 1959). The effects of the helix angle, the interwire friction moments and friction forces are shown in Figs. 10, 11 and 12, respectively. Smaller helix angles will cause more energy dissipation, and so will the smaller friction forces and moments. These results are in correspondence with the effects of these parameters on the slipping length given by Eq. (53).

4. Conclusion

A mathematical model of a cable as a system of interacting wires is developed. The model allows to analyze the energy dissipation during the process of cable extension, and the effect of dry friction on this process. The following main results are briefly summarised:

(1) Explicit expression for the energy dissipation caused by dry friction is derived. It shows that the energy dissipation is proportional to the cube of the tensile load and in inverse proportion to the friction forces, which is a typical characteristic of losses in dry friction joints. Other structural parameters including the wire number and helix angles also affect the energy dissipation.

(2) The energy dissipation is caused by the twisting and bending deformations of wires.

(3) The process of cable extension is accompanied by the processes of micro-slippage due to the rotation of the wire along the normal to the core at the contact patches, and macro-slippage due to the twisting and bending of the wire with respect to the tangential and bi-normal directions of the helix.

(4) In the part of the cable where slippage takes place, the helix angle is not constant but varies as a linear function of the longitudinal coordinate.

(5) The stiffness of the cable with finite friction forces is weakly nonlinear.

(6) The model was evaluated by comparing it with the experimental results obtained by Utting and Jones (1987), and a frictionless model according to Costello (1990). It is shown that the results for a model with finite friction forces are bounded by the results for the two extremes cases: friction-free and infinite friction models.

Acknowledgements

The financial support provided by the Natural Sciences and Engineering Research Council of Canada in the form of an operating grant is gratefully acknowledged.

References

Cappa, P. (1987), "An experimental study of wire strains in an undamaged and damaged steel strand subjected to tensile load", *Exp. Mech., Dec.*, 346-349.

Casey, N. F., and Lee, W. K.(1989), "The fatigue failure of large diameter six strand wire rope", *Int. J. Fatigue*, **11**(2), 78-84.

Chi, M. (1974), "Analysis of multi-wire strands in tension and combined tension and torsion", Developme-

nts in Theoretical and Applied Mechanics, *Proceedings of the Seventh Southeastern Conference on Theoretical and Applied Mechanics*, 599-639.

Claren, R., and Diana, G. (1969), "Mathematical analysis of transmission line vibration", *IEEE Transaction on Power Apparatus and Systems,* **88**(12), 1741-1767.

Costello, G. A. (1990), *Theory of Wire Rope,* New York: Springer-Verlag.

Goodman, L. E. (1959), "A review of progress in analysis of interfacial slip damping", *Structural Damping,* Ruzicka, J.E. ed., *ASME*, New York, 35-48.

Huang, N. C.(1973), "Theories of elastic slender curved rods", *ZAMP*, **24**, 1-19.

Huang, N. C. (1978), "Finite extension of an elastic strand with a central core", *J. of Applied Mechanics, ASME,* **44**, 852-858.

Huang, X. and Vinogradov, O.G. (1992), "Interwire slip and its influence on the dynamic properties of tension cables", *2nd Int. Offshore and Polar Engineering Conference,* Paper No.ISOPE-92-T5-01, San Francisco, June 14-19.

Huang, X., and Vinogradov, O. (1994), "Analysis of dry friction hysteresis in a cable under uniform bending", *Structural Engineering and Mechanics,* **2**(1), 63-80.

LeClair, R. A., and Costello, G. A. (1988), "Axial, bending and torsional loading of strand with friction", *J. of Offshore Mech. and Arctic. Engrg. , ASME,* **110**, 38-42.

Love, A. E. H. (1944), *A treatise on the mathematical theory of elasticity,* New York: Dover Publications.

Knapp, R. H.(1979), "Derivation of a new stiffness matrix for helically armoured cable considering tension and torsion", *Int. J. Numer. Mech. Engrg.,* **14**, 515-529.

Kumar, K., and Cochran, J. E. Jr. (1987), "Closed-form analysis for elastic deformations of multilayered strands", *J. of Applied Mechanics, ASME,* **54**, 898-903.

Machida, S., and Durelli, A. J. (1973), "Response of a strand to axial and torsional displacements", *J. of Mech. Eng. Sci.,* **15**, 241-251.

Phillips, J. W., and Costello, G. A. (1973), "Contact stresses in twisted wire cables", *J. of Eng. Mech., ASCE,* **99**, 331-341.

Pipes, L. A. (1936), "Cable and damper vibration studies", *AIEE Transactions,* **55**, 600-614.

Pivovarov, I., and Vinogradov, O. G. (1985), "The Phenomenon of damping in stranded cables", *Proceedings of 26th SDM Conference,* Part 2, Orlando, U.S.A., 232-237.

Ramsey, H. (1990), "Analysis of interwire friction in multilayered cables under uniform extension and twisting" *Int. J. Mech. Sci.,* **32**(8), 709-716.

Utting, W. S., and Jones, N. (1987a), "The response of wire rope strands to axial tensile loads part I: Experimental results and theoretical predictions", *Int. J. Mech. Sci.,* **29**(9), 605-619.

Vinogradov, O. and Huang, X. (1991), "Dry friction losses in an axially deformed stranded cable", *1991 ASME Pressure Vessel & Piping Conference,* PVP-Vol. **211**, San Diego, USA, June 23-27.

Vinogradov, O., and Atatekin, I.S. (1986), "Internal friction due to twist in bent cable", *J. of Engrg. Mech., ASCE,* **112**(9), 859-873.

Vranish, J. M. (1990), "Advanced mechanisms for robotics", NASA Conference Publication, 3109, **1**, *Technology 2000,* November 27-28.

Yu, A. (1952), "Vibration damping of stranded cable", *Proc. Soc. Exp. Stress Analysis,* **9**, 141-158.